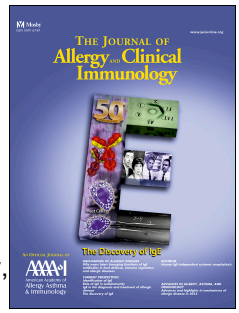
Accepted Manuscript



B cells differentiate in Human thymus and express AIRE

Vincent Gies, PhDs, Aurélien Guffroy, MD, François Danion, MD, Philippe Billaud, MD, Céline Keime, PhD, Jean-Daniel Fauny, PhD, Sandrine Susini, PhD, Anne Soley, LT, Thierry Martin, MD, PhD, Jean-Louis Pasquali, MD, PhD, Frédéric Gros, PhD, Isabelle André-Schmutz, PhD, Pauline Soulas-Sprauel, PharmD, PhD, Anne-Sophie Korganow, MD, PhD

PII: S0091-6749(16)31295-7

DOI: 10.1016/j.jaci.2016.09.044

Reference: YMAI 12450

To appear in: *Journal of Allergy and Clinical Immunology*

Received Date: 1 March 2016

Revised Date: 18 August 2016

Accepted Date: 5 September 2016

Please cite this article as: Gies V, Guffroy A, Danion F, Billaud P, Keime C, Fauny J-D, Susini S, Soley A, Martin T, Pasquali J-L, Gros F, André-Schmutz I, Soulas-Sprauel P, Korganow A-S, B cells differentiate in Human thymus and express AIRE, *Journal of Allergy and Clinical Immunology* (2016), doi: 10.1016/j.jaci.2016.09.044.

This is a PDF file of an unedited manuscript that has been accepted for publication. As a service to our customers we are providing this early version of the manuscript. The manuscript will undergo copyediting, typesetting, and review of the resulting proof before it is published in its final form. Please note that during the production process errors may be discovered which could affect the content, and all legal disclaimers that apply to the journal pertain.

ACCEPTED MANUSCRIPT

B cells differentiate in Human thymus and express AIRE

Journal of Allergy and Clinical Immunology

Section designation: Letter to the Editor

Vincent Gies, PhDs,[a,b] Aurélien Guffroy, MD,[a,b]* François Danion, MD,[a,b]* Philippe Billaud, MD,[c] Céline Keime, PhD,[d] Jean-Daniel Fauny, PhD,[a] Sandrine Susini, PhD,[e] Anne Soley, LT,[a] Thierry Martin, MD, PhD,[a,b,f] Jean-Louis Pasquali, MD, PhD,[a,b,f] Frédéric Gros, PhD,[a,g] Isabelle André-Schmutz, PhD,[e]** Pauline Soulas-Sprauel, PharmD, PhD,[a,b,h]** Anne-Sophie Korganow, MD, PhD,[a,b,f]

[a]CNRS UPR 3572 "Immunopathology and Therapeutic Chemistry"/Laboratory of Excellence Medalis, Institute of Molecular and Cellular Biology (IBMC), Strasbourg, France.

[b]Department of Clinical Immunology and Internal Medicine, National Reference Center for Autoimmune Diseases, Hôpitaux Universitaires de Strasbourg, Strasbourg, France.

[c]Department of Cardiovascular Surgery, Hôpitaux Universitaires de Strasbourg, Strasbourg, France.

[d]IGBMC (Institut de Génétique et de Biologie Moléculaire et Cellulaire), INSERM, U964, CNRS, UMR7104, Université de Strasbourg, Illkirch, France.

[e]INSERM, U1163, Université Paris Descartes, Sorbonne Paris Cité, Institut Imagine, Paris, France.

[f]UFR Médecine, Université de Strasbourg, Strasbourg, France.

[g]Faculté des Sciences de la Vie, Université de Strasbourg, Strasbourg, France.

[h]UFR Sciences pharmaceutiques, Université de Strasbourg, Illkirch-Graffenstaden, France.

*A.G. and F.D. contributed equally to the work.

**I.A.S. and P.S.S contributed equally to the work

Correspondence:

Prof. Anne-Sophie Korganow, MD PhD

CNRS UPR 3572 “Immunopathology and Therapeutic Chemistry”

Institute of Molecular and Cellular Biology (IBMC)

15 rue René Descartes, 67084 Strasbourg Cedex, FRANCE

Telephone number: + 33 3 88 41 70 25

Fax: + 33 3 88 61 06 80

E-mail address: korganow@unistra.fr

Conflict-of-interest disclosure:

The authors declare no competing financial interests.

ACCEPTED MANUSCRIPT

AUTHORSHIP

Contributions:

V.G., T.M., J.L.P., F.G., I.A.S., P.S.S. and A.S.K. designed the research.

V.G., A.G., F.D., P.B.,C.K., S.S., J.D.F. and A.S. performed the research.

V.G, T.M., J.L.P., F.G., J.D.F., C.K., I.A.S., P.S.S. and A.S.K. analyzed the data.

V.G., F.G., F.D., A.G., I.A.S., P.S.S. and A.S.K. wrote the paper.

TEXT COUNT

Words number: 1366

Figures number: 2 (+5 supplemental)

Table number: 2 supplemental

Supplemental number: 1 method, 2 tables, 5 figures

ACCEPTED MANUSCRIPT

CAPSULE SUMMARY / KEY MESSAGES

- All B cell differentiation stages are represented in human thymus with proliferating precursors suggesting intrathymic differentiation.
- Thymic mature B cells present an APC phenotype, express AIRE and genes coding for TRAs.

KEY WORDS

B cells; Human thymus; phenotype; AIRE; APC; TRAs

ABBREVIATIONS

AIRE: Autoimmune Regulator (Human protein)

AIRE: Autoimmune Regulator (Human gene)

Aire: Autoimmune regulator (mice protein)

Aire: Autoimmune regulator (mice gene)

APC: Antigen Presenting Cell

BM: Bone marrow

CD40L: CD40 Ligand

MHCII: Major Histocompatibility class II

mTEC: medullary Thymic Epithelial Cell

P1: Patient 1

PB: Peripheral Blood

PBMC: Peripheral Blood Mononuclear cell

sIg: Surface Immunoglobulin

ACCEPTED MANUSCRIPT

TRA: Tissue Restricted Antigen

To the Editor:

It has been known for more than a decade that human thymus contains a minor contingent of B cells.[1] Some authors suggested that these B cells reflect the homing of peripheral B cells, others wondered if they could act as antigen presenting cells (APCs). Recently, two important papers approached the role of thymic B cells in murine models, using transfer experiments and deficient lines (e.g: Aire knock-out animals). They demonstrated that murine B cells are potent APCs to autoreactive T cells[2] and that they can harbor different self tissue restricted antigens (TRAs) induced by autoimmune regulator (Aire) expression.[3] But only little is known about human B cells fate and function in thymus with mostly immunochemistry data.[1] Considering this critical issue, we explored the phenotype of B cells from thymuses of young donors undergoing heart surgery (see Table E1 and the Methods section in this article's Online Repository at www.jacionline.org).

$CD19^+$ B cells were detected in the medulla and throughout the cortex (Fig 1, *A*), while IgM^+ B cells were restricted to the medulla and the cortico-medullary junction (Fig 1, *B* and *C).* B cells constituted 0.92%±0.23 of thymic lymphocytes (see Fig E1, *A*). All developmental stages (see

Fig E2) were represented, from pro-B cells to differentiated B cells, and mature naive B cells were largely predominant (48.53%±3.15, Fig 1, *D*, and see Fig E1, *B*). Both switched $CD27^-$ and $CD27^+$ memory B cells were present (Fig 1, *D*). Further analysis of the surface immunoglobulin (sIg) expression showed that they were mainly IgG with less IgA expression. Plasmablast subset was enriched in sIgM with a low level of sIgG or sIgA (Fig 1, *E*). $CD27^+$ switched B cells result of antigen recognition in germinal centers or in mucosal tissues.[4] $CD27^-$ switched B cells are low mutated and have been suspected to be a reservoir of autoreactive B cells (IgG^+) or involved in the maintenance of intestinal homeostasis (IgA^+).[5] Thus, it is interesting to note that all these B cell subsets are present in the thymus in significant proportions.

Obviously thymic B cell phenotype was different from BM picture, with a clear predominance of precursors in BM and of mature naïve B cells in the thymus. In addition, switched memory B cell numbers were very low in BM, but represented around 15% of thymic B cells.

We were able to compare B cell subpopulations in thymus, bone marrow (BM) and peripheral blood (PB) from a single donor (P1). The repartition of the different B cell subpopulations in BM and blood for our patient was consistent with literature data. The thymic B cell picture was also distinct from PB, as there were more precursors and mature naive B cells in the thymus (see Fig E3, *A, B* and *C*). These findings do not support the hypothesis of a peripheral B cells homing.

In thymuses, immature B cells proliferated more than mature subsets (70.96%±4.00 vs. 46.94%±3.05) (Fig 2, *A*). Both the proliferation of B cell progenitors in the thymus and their higher frequency compared to PB, argue for in situ B cell lymphopoiesis.

We hypothesized that thymic B cells could harbor an organ specific function. Mature thymic B cells ($CD19^+CD10^-$) expressed higher levels of major histocompatibility class II (MHCII) levels compared to immature B cells ($CD19^+CD10^+$) (Fig 2, *B*). CD40 expression was detected on

87.6% of mature thymic B cells, whereas being barely detectable on immature B cells (Fig 2, *C*). CD86 was not expressed on immature B cells but upregulated on 28.9% of $CD19^{+}CD10^{-}$ B cells (Fig 2, *D*). In further distinction from B cells in other organs, in the same individual, this CD86 upregulation was only observed in mature thymic B cells, but neither in immature or mature B cells from BM or PB (see Fig E3, *D*). In mice the thymic B cell licensing is driven through CD40-CD40L signaling and interaction with $CD4^{+}$ T cells.[3,6] Here, mature thymic B cells expressed MHCII molecules and CD86 concomitantly with CD40 expression, which could reflect similar mechanisms of activation. In addition, 18.8% of thymic B cells expressed CD5, with an expression restricted to $CD19^{+}CD10^{-}$ (Fig 2, *E*), similar to BM B cells, but at a lower level than in PB (see Fig E3, *E*). In mice, treatment of B2b B cell with anti-IgM and CD40 stimulation induced CD5 expression at low level.[7] A role of CD40-CD40L interaction in human thymic B cells activation could explain the CD5 expression on some of them.

The fact that (i) human thymic B cells are localized mainly in the medulla and at the cortico-medullary junction, (ii) mature thymic B cells strongly express MHCII molecules and CD86, suggest that they could act as APCs.

These data prompted us to explore if they could present auto-antigens to T cells, as recently demonstrated in mice.[2,3] Using immunofluorescence analysis, we detected AIRE protein with typical punctuate nuclear staining in TECs (27.05%±2.07) and also, yet with less numerous nuclear dots, in thymic B cells ($CD19^{+}$: 5.58%±1.59, IgM^{+}: 6.69%±0.83) (Fig 2, *F* and see Fig E4). In addition, the most predominant thymic B cell subset ($CD27^{-}IgM^{+}$), expressed 80 fold more *AIRE* mRNA than thymocytes (Fig 2, *G*). If relevant, AIRE expression in thymic B cells may repress or induce the expression of other genes, as the induction of TRAs expression in medullary thymic epithelial cells (mTECs).[8] Little is known about the nature of TRAs expressed

by murine thymic B cells, and there is only a very limited overlap of TRAs between mTECs and extrathymic Aire-expressing cells,[3] suggesting that thymic B cells may regulate expression of a unique set of TRAs. Using the thymic B cells' TRAs (see the Methods section in this article's Online Repository) defined by Yamano et al.,[3] we detected a significant expression of *CDH17* and *LAMP3* – representative TRAs of the intestinal tract and the lung, respectively – concomitantly with a lower expression of *KLRB1*, an Aire-repressed gene (Fig 2, *H*). We were not able to detect *GRIK2* or *SCEL* expression. We performed RNAseq analysis on sorted $CD19^{+}IgM^{+}CD27^{-}$ thymic B cells, this analysis confirmed our qRT-PCR results including AIRE overexpression (fold change: 4.82, p-value = $6.53.10^{-5}$). Moreover, thymic B cells expressed more TRA genes than peripheral B cells (168 TRA genes upregulated vs 48 repressed). Each TRA is only expressed by 1-3% of mTECs at a given time.[8] In addition as only 5% of thymic B cells are AIRE positive, the number of TRA genes expressed by AIRE positive thymic B cells may be even higher. Some of these TRAs have been associated to autoimmune diseases, for example LAD1 (linear IgA dermatosis), SCG2 (autoimmune hypophysitis), ICA1 (type 1 diabetes), ACHE and AKAP12 (myasthenia gravis) or METRNL (autoimmune hepatitis) (Fig 2, *I* and see Table E2).

Interestingly, some molecules of the LAMP family, being associated with the lysosomal membrane, play an essential role in autophagy.[9] This process is involved in providing endogenous self-peptides for MHCII presentation and plays a role in thymocytes selection provided by TECs.[8] We found equivalent expression of *BECN1* – initiation of the autophagosome formation – between thymic $CD19^{+}CD27^{-}IgM^{+}$ and PB $CD19^{+}CD27^{-}IgM^{+}$, while *ATG5* expression – elongation of the autophagosomal membrane – was reproducibly lower in thymus. Similar results were found in RNAseq (not shown) and we cannot conclude at this

stage about the involvement of autophagic activity in thymocyte education by B cells.

In this study, we confirm the presence of both immature and mature B cells in the thymuses of young donors. Although some B cells progenitors are present and proliferate likely in the cortex, most B cells in the thymus are mature B cells with an APC phenotype, located to the medulla. The analysis of AIRE and TRA genes expression support the hypothesis of their involvement in negative selection and suggest a new layer of complexity in the process of human central tolerance. Indeed, it will be of great interest to go further, but it is a challenging issue considering the low percentages of B cells in this organ. Primary immunodeficiencies affecting B cells include autoimmune manifestations in their clinical presentation. The mechanisms of this autoimmunity remain unclear and can be organ specific. In view of our results, it is reasonable to assume that in some cases central T cell tolerance mediated by B cells could be affected**.**

ACCEPTED MANUSCRIPT

ACCEPTED MANUSCRIPT

ACKNOWLEDGMENTS

We thank C. Herouard-Molina (IGBMC, Illkirch, France) for expert technical assistance for the whole transcriptome sequencing. Sequencing was performed by the GenomEast platform, a member of the “France Génomique” consortium (ANR-10-INBS-0009). We thank E. Meffre (Department of Immunobiology, Yale University School of Medicine, New Haven, USA) and M. Van Zelm (Department of Immunology and Pathology, Central Clinical School, Monash University, Melbourne, Australia) for helpful discussion.

ACCEPTED MANUSCRIPT

ACCEPTED MANUSCRIPT

Vincent Gies, PhDs,[a,b]
Aurélien Guffroy, MD,[a,b]*
François Danion, MD,[a,b]*
Philippe Billaud, MD,[c]
Céline Keime, PhD,[d]
Jean-Daniel Fauny, PhD,[a]
Sandrine Susini, PhD,[e]
Anne Soley, LT,[a]
Thierry Martin, MD, PhD,[a,b,f]
Jean-Louis Pasquali, MD, PhD,[a,b,f]
Frédéric Gros, PhD,[a,g]
Isabelle André-Schmutz, PhD,[e]**
Pauline Soulas-Sprauel, PharmD, PhD,[a,b,h]**
Anne-Sophie Korganow, MD, PhD,[a,b,f]

[a]CNRS UPR 3572 "Immunopathology and Therapeutic Chemistry"/Laboratory of Excellence Medalis, Institute of Molecular and Cellular Biology (IBMC), Strasbourg, France.
[b]Department of Clinical Immunology and Internal Medicine, National Reference Center for Autoimmune Diseases, Hôpitaux Universitaires de Strasbourg, Strasbourg, France.
[c]Department of Cardiovascular Surgery, Hôpitaux Universitaires de Strasbourg, Strasbourg, France.

[d]IGBMC (Institut de Génétique et de Biologie Moléculaire et Cellulaire), INSERM, U964, CNRS, UMR7104, Université de Strasbourg, Illkirch, France.

[e]INSERM, U1163, Université Paris Descartes, Sorbonne Paris Cité, Institut Imagine, Paris, France.

[f]UFR Médecine, Université de Strasbourg, Strasbourg, France.

[g]Faculté des Sciences de la Vie, Université de Strasbourg, Strasbourg, France.

[h]UFR Sciences pharmaceutiques, Université de Strasbourg, Illkirch-Graffenstaden, France.

*A.G. and F.D. contributed equally to the work.

**I.A.S. and P.S.S contributed equally to the work

LEGENDS

FIG 1. A, B and **C,** Thymus immunostaining with anti-CD19 (Fig 1, A) or anti-IgM (Fig 1, B and C) antibody (*red*). medulla *(m)*; cortex *(c);* DAPI *(grey)*. **D,** B cells subsets (percentages of $CD19^+$ cells) in thymus ($n \geq 4$) and BM ($n = 3$). Antibodies mentioned on axes are applied to the population defined on the top of each plot. **E,** Isotype frequency in sIg^+ switched thymic B cells ($n = 4$).

FIG 2. A, B, C, D and **E,** MFI (*black*) and isotypic controls (*grey*), on thymic B cells ($n \geq 4$). **F,** AIRE protein (*green*) in TECs and in $CD19^+$ or IgM^+ (*red*) thymic B cells. **G,** *AIRE* expression in thymocytes ($n = 6$) and thymic B cells ($n = 5$). **H,** AIRE-related genes and genes involved in autophagy, in thymic B cells ($n = 5$) compared to their peripheral counterpart ($n = 4$). *CDH17* remained undetectable in periphery, except for one sample. **I,** Graphical representation of RNA sequencing data. *AIRE* (*blue*); TRAs associated to autoimmune diseases (*red*).*$P<.05$, **$P<.005$.

REFERENCES

1. Isaacson PG, Norton AJ, Addis BJ. The human thymus contains a novel population of B lymphocytes. Lancet 1987;2:1488–91.

2. Perera J, Meng L, Meng F, Huang H. Autoreactive thymic B cells are efficient antigen-presenting cells of cognate self-antigens for T cell negative selection. Proc Natl Acad Sci U S A 2013;110:17011–6.

3. Yamano T, Nedjic J, Hinterberger M, Steinert M, Koser S, Pinto S, et al. Thymic B Cells Are Licensed to Present Self Antigens for Central T Cell Tolerance Induction. Immunity 2015;42:1048–61.

4. Berkowska MA, Driessen GJA, Bikos V, Grosserichter-Wagener C, Stamatopoulos K, Cerutti A, et al. Human memory B cells originate from three distinct germinal center-dependent and -independent maturation pathways. Blood 2011;118:2150–8.

5. Berkowska MA, Schickel J-N, Grosserichter-Wagener C, Ridder D de, Ng YS, Dongen JJM van, et al. Circulating Human CD27−IgA+ Memory B Cells Recognize Bacteria with Polyreactive Igs. J Immunol 2015;1402708.

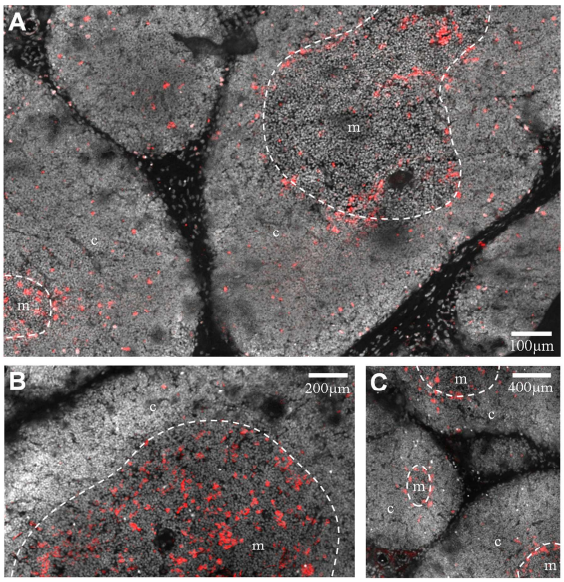
6. Fujihara C, Williams JA, Watanabe M, Jeon H, Sharrow SO, Hodes RJ. T cell-B cell thymic cross-talk: maintenance and function of thymic B cells requires cognate CD40-CD40 ligand interaction. J Immunol Baltim Md 1950 2014;193:5534–44.

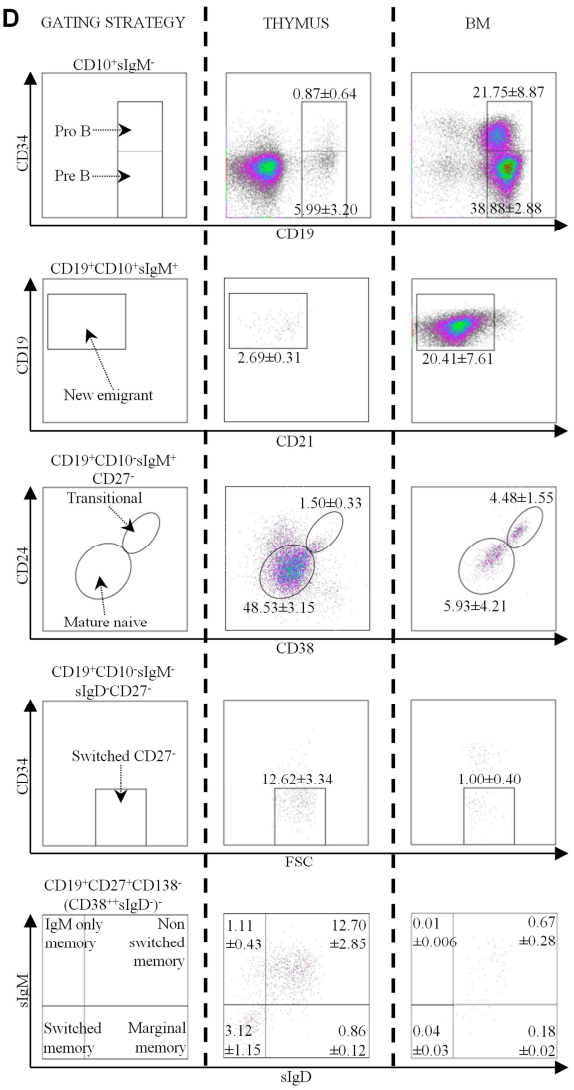
7. Wortis HH, Teutsch M, Higer M, Zheng J, Parker DC. B-cell activation by crosslinking of surface IgM or ligation of CD40 involves alternative signal pathways and results in different B-cell phenotypes. Proc Natl Acad Sci U S A 1995;92:3348–52.

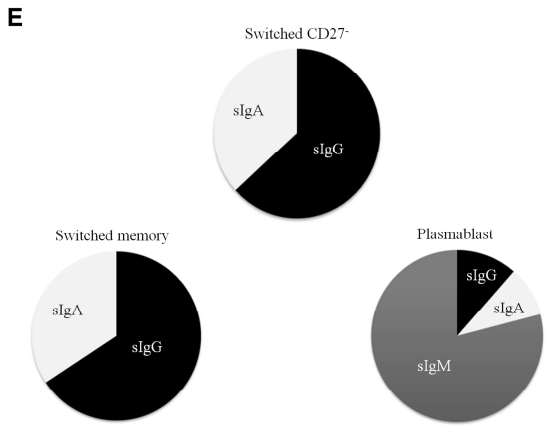
8. Klein L, Kyewski B, Allen PM, Hogquist KA. Positive and negative selection of the T cell repertoire: what thymocytes see (and don't see). Nat Rev Immunol 2014;14:377–91.

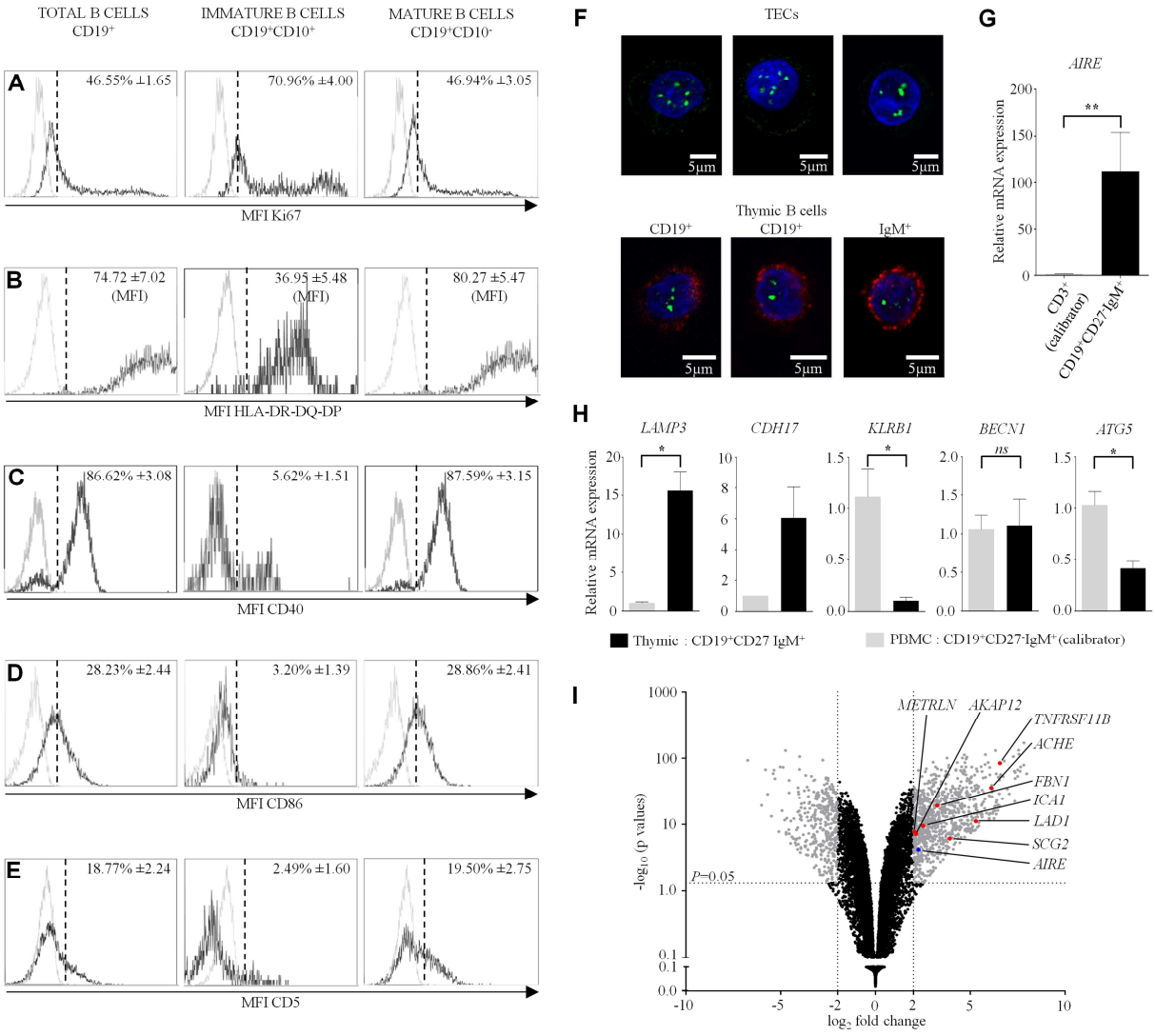
9. Tanaka Y, Guhde G, Suter A, Eskelinen EL, Hartmann D, Lüllmann-Rauch R, et al. Accumulation of autophagic vacuoles and cardiomyopathy in LAMP-2-deficient mice. Nature 2000;406:902–6.

ACCEPTED MANUSCRIPT


A
m
c
c
m
100μm
B
200μm
c
m
C
400μm
m
c
m
c
c
m


D
GATING STRATEGY
THYMUS
BM
CD10+sIgM-
Pro B
Pre B
CD34
CD19
0.87±0.64
5.99±3.20
21.75±8.87
38.88±2.88
CD19+CD10+sIgM+
New emigrant
CD19
CD21
2.69±0.31
20.41±7.61
CD19+CD10-sIgM+ CD27-
Transitional
Mature naive
CD24
CD38
1.50±0.33
48.53±3.15
4.48±1.55
5.93±4.21
CD19+CD10-sIgM- sIgD-CD27-
Switched CD27-
CD34
FSC
12.62±3.34
1.00±0.40
CD19+CD27+CD138- (CD38++sIgD-)-
IgM only memory
Non switched memory
Switched memory
Marginal memory
sIgM
sIgD
1.11 ±0.43
12.70 ±2.85
3.12 ±1.15
0.86 ±0.12
0.01 ±0.006
0.67 ±0.28
0.04 ±0.03
0.18 ±0.02


E
Switched CD27-
sIgA
sIgG
Switched memory
sIgA
sIgG
Plasmablast
sIgG
sIgA
sIgM


TOTAL B CELLS
CD19+
IMMATURE B CELLS
CD19+CD10+
MATURE B CELLS
CD19+CD10-
A
46.55% ±1.65
70.96% ±4.00
46.94% ±3.05
MFI Ki67
B
74.72 ±7.02
(MFI)
36.95 ±5.48
(MFI)
80.27 ±5.47
(MFI)
MFI HLA-DR-DQ-DP
C
86.62% ±3.08
5.62% ±1.51
87.59% ±3.15
MFI CD40
D
28.23% ±2.44
3.20% ±1.39
28.86% ±2.41
MFI CD86
E
18.77% ±2.24
2.49% ±1.60
19.50% ±2.75
MFI CD5
F
TECs
5µm
Thymic B cells
CD19+
CD19+
IgM+
G
AIRE
Relative mRNA expression
**
CD3+ (calibrator)
CD19+CD27-IgM+
H
LAMP3
CDH17
KLRB1
BECN1
ATG5
Relative mRNA expression
*
ns
Thymic : CD19+CD27 IgM+
PBMC : CD19+CD27-IgM+ (calibrator)
I
METRLN
AKAP12
TNFRSF11B
ACHE
FBN1
ICA1
LAD1
SCG2
AIRE
P=0.05
-log10 (p values)
log2 fold change

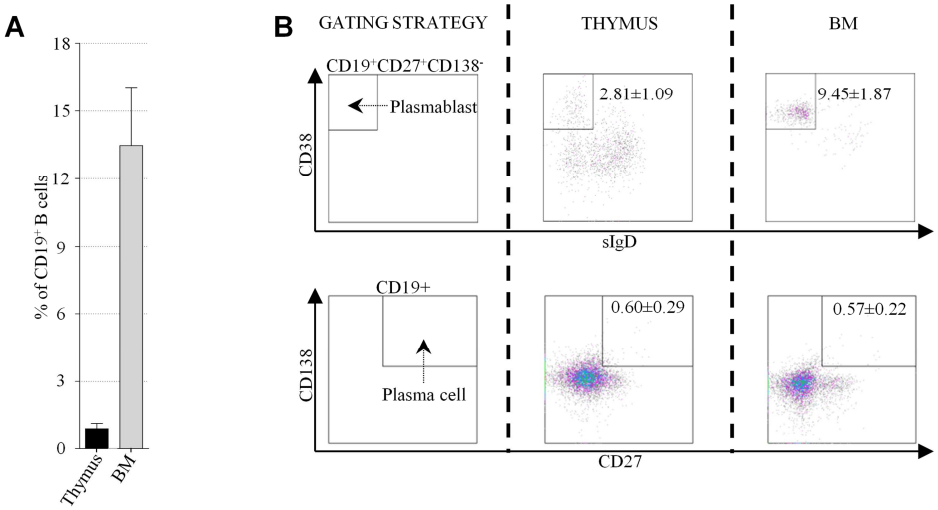
ACCEP

TABLE E1. Clinical features of the subjects included in the study. Thymuses from Patient 1 (P1) to P8 were collected. For P1, PB and BM were also available. For P9 and P10, only BM was available.

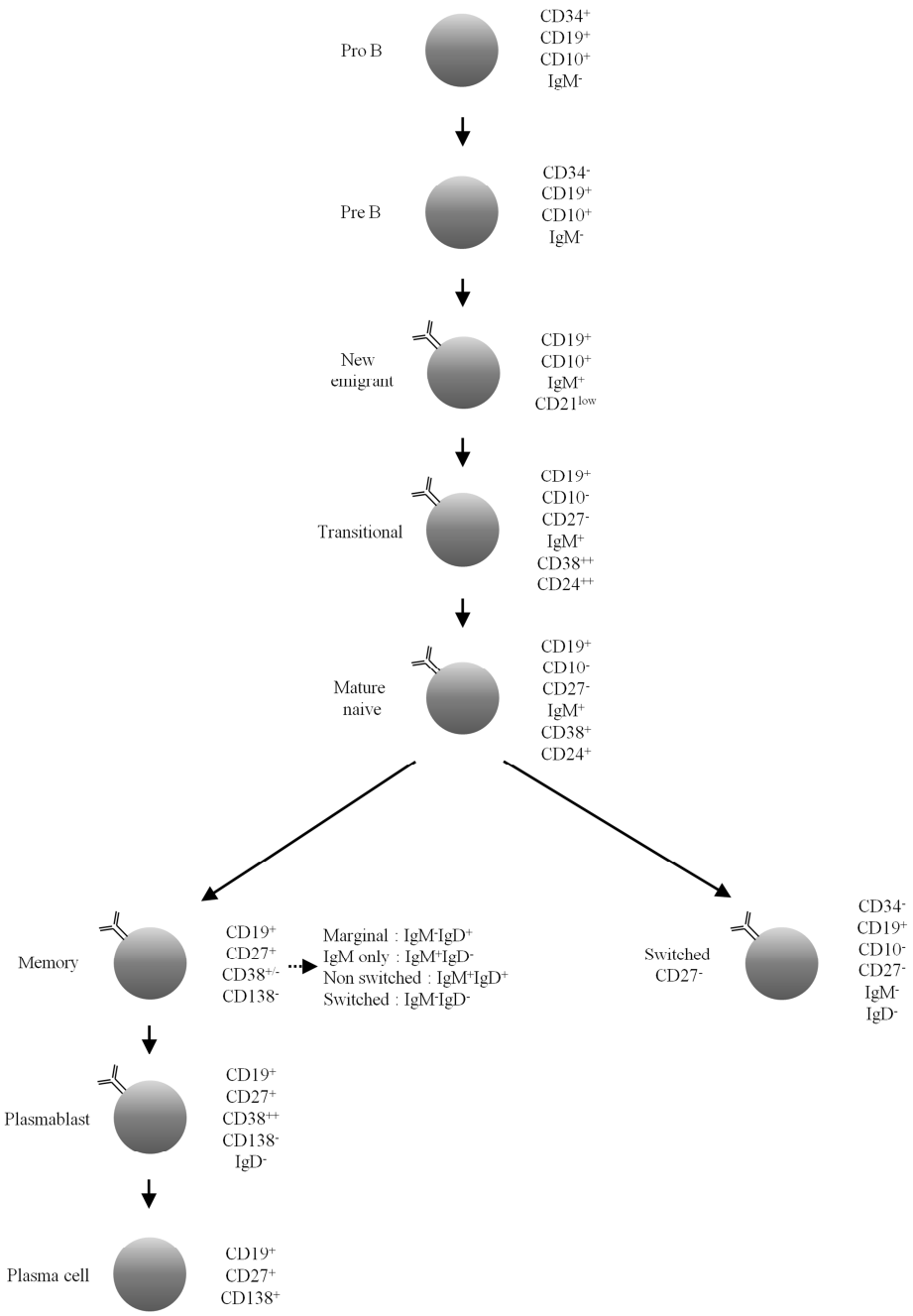
Patients	Sex	Age (weeks)	Cause of surgery
P1	Male	1	Tricuspid atresia
P2	Male	2	TGV[a]
P3	Female	26	Tetralogy of Fallot
P4	Male	2	TGV[a]
P5	Female	14	IAC[b]-IVC[c]
P6	Male	1	TAPVR[d]
P7	Female	1	TGA + IVC
P8	Male	3	DORV[e]
P9	Male	3	Shone's syndrome
P10	Male	1	PAIVS[f]

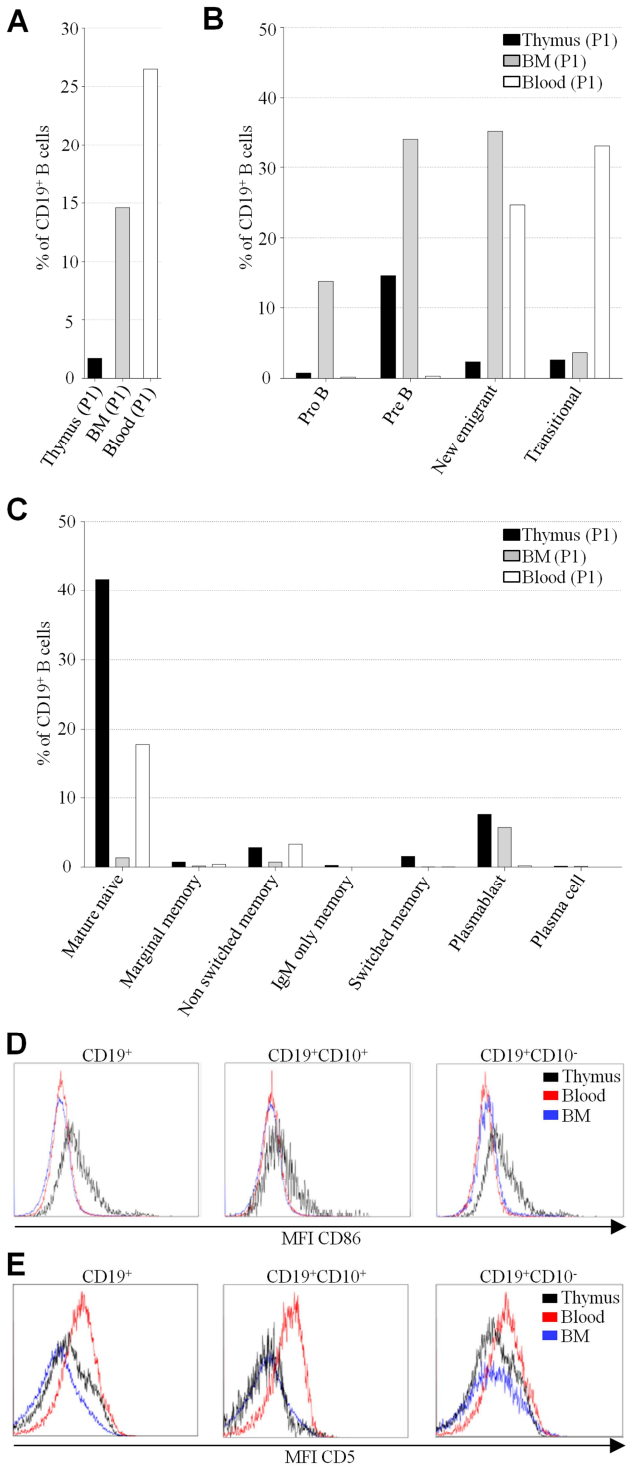
[a]Transposition of Great Vessels
[b]Inter-Atrial Communication
[c]Inter-Ventricular Communication
[d]Total Anomalous Pulmonary Venous Return
[e]Double Outlet Right Ventricle
[f]Pulmonary Atresia with Intact Ventricular Septum

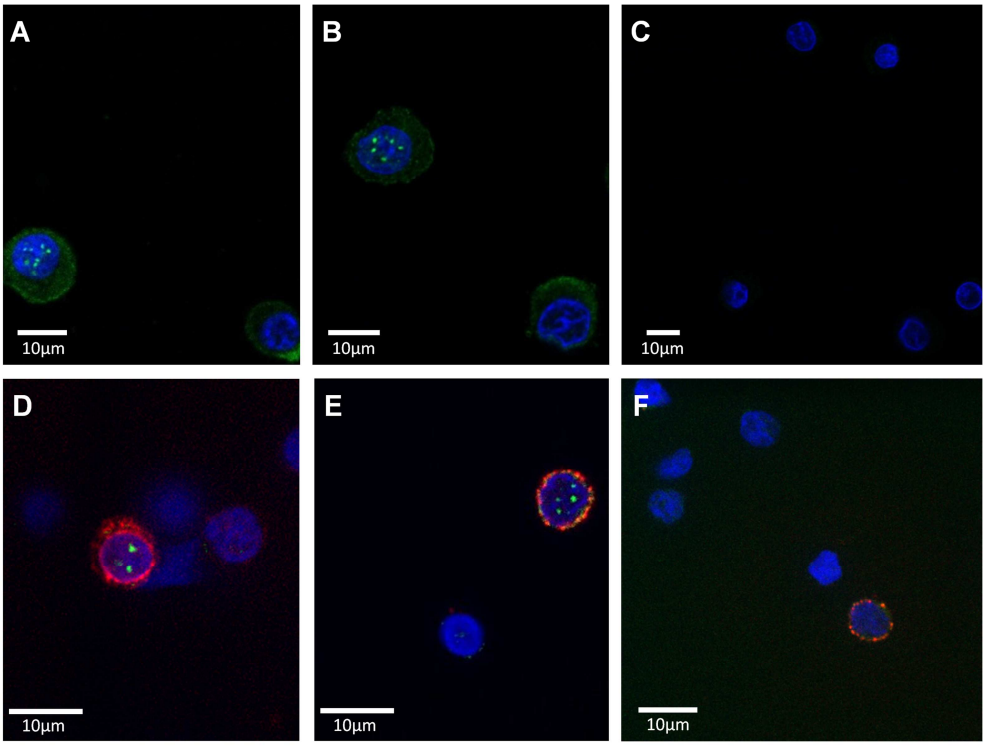
ACCEPTED MANUSCRIPT



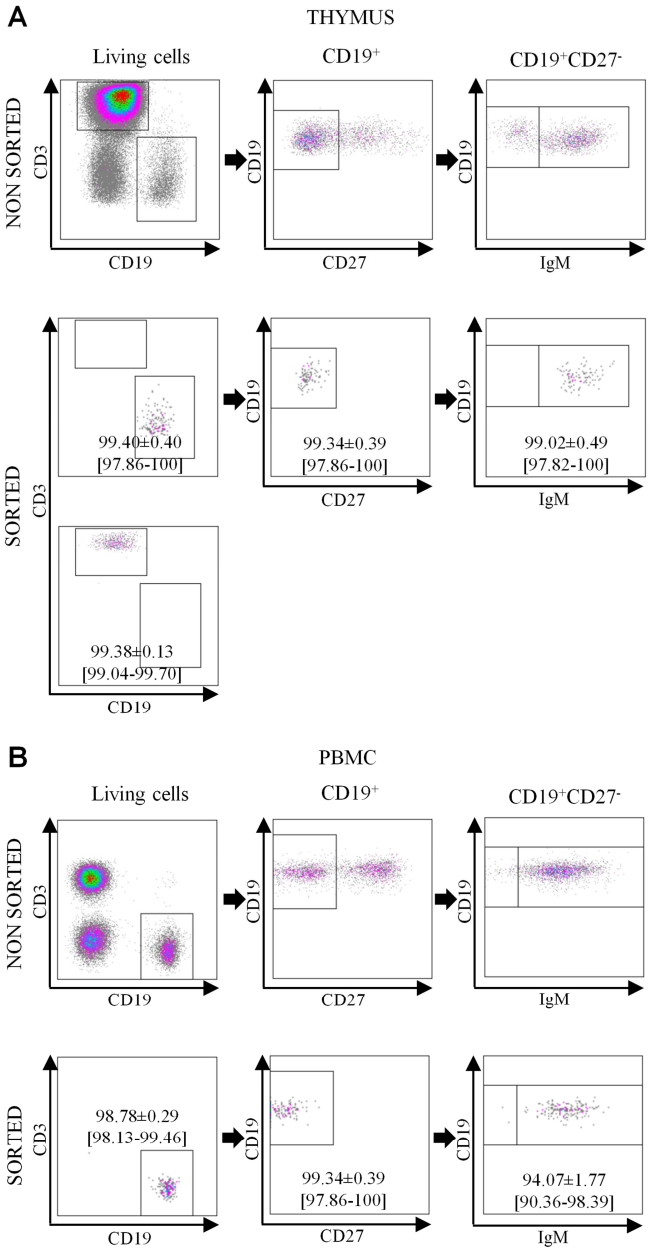
ACCEPTED MANUSCRIPT


Pro B
CD34+
CD19+
CD10+
IgM-
Pre B
CD34-
CD19+
CD10+
IgM-
New emigrant
CD19+
CD10+
IgM+
CD21low
Transitional
CD19+
CD10-
CD27-
IgM+
CD38++
CD24++
Mature naive
CD19+
CD10-
CD27-
IgM+
CD38+
CD24+
Memory
CD19+
CD27+
CD38+/-
CD138-
Marginal : IgM-IgD+
IgM only : IgM+IgD-
Non switched : IgM+IgD+
Switched : IgM-IgD-
Switched CD27-
CD34-
CD19+
CD10-
CD27-
IgM-
IgD-
Plasmablast
CD19+
CD27+
CD38++
CD138-
IgD-
Plasma cell
CD19+
CD27+
CD138+


A
% of CD19+ B cells
Thymus (P1)
BM (P1)
Blood (P1)
B
% of CD19+ B cells
Thymus (P1)
BM (P1)
Blood (P1)
Pro B
Pre B
New emigrant
Transitional
C
% of CD19+ B cells
Thymus (P1)
BM (P1)
Blood (P1)
Mature naive
Marginal memory
Non switched memory
IgM only memory
Switched memory
Plasmablast
Plasma cell
D
CD19+
CD19+CD10+
CD19+CD10-
Thymus
Blood
BM
MFI CD86
E
CD19+
CD19+CD10+
CD19+CD10-
Thymus
Blood
BM
MFI CD5



ACCEPTED MANUSCRIPT


A
THYMUS
Living cells
CD19+
CD19+CD27-
NON SORTED
SORTED
CD3
CD19
CD27
IgM
99.40±0.40
[97.86-100]
99.34±0.39
[97.86-100]
99.02±0.49
[97.82-100]
99.38±0.13
[99.04-99.70]
B
PBMC
Living cells
CD19+
CD19+CD27-
98.78±0.29
[98.13-99.46]
99.34±0.39
[97.86-100]
94.07±1.77
[90.36-98.39]

ACCEPTED MANUSCRIPT

METHODS

Patients and samples

The study was conducted in accordance with the principles of the Helsinki declaration. Informed consent was obtained from the parents or legal wards of the patients and the study protocol was approved by the Clinical Research Ethics Committee of Strasbourg's University Hospital.

Anticoagulated venous blood from 4 healthy donors was collected and was subjected to density gradient centrifugation with LSM1077 (GE Healthcare Life Sciences, Velizy-Villacoublay, France) to get peripheral blood mononuclear cells (PBMC) and remove dead cells.

Thymus glands were collected after thymectomy of infants undergoing corrective heart surgery in the Department of Pediatric Surgery (Strasbourg's University Hospital). Patients affected by diseases or receiving treatments that may alter the immunological system were excluded, namely primary immunodeficiencies, active bacterial or viral infections, chronic viral infections, chemotherapy or neoplasms. None of them was affected with Down syndrome or other evident dysmorphic features. Their ages ranged from 1 week to 26 weeks. The main characteristics of patients are described in Table E1 in the Online Repository at www.jacionline.org. Pieces of thymuses from patient 1 (P1) were embedded in O.C.T. (Tissue-Tek, Sakura, Torrance, CA, USA) and stored at -80°C for immunofluorescence microscopy experiments. Thymus cellular suspensions were obtained by grinding the organ on a 40µm cell strainer (BD Falcon, Franklin Lakes, NJ, USA). Thymic and BM cells were subjected to density gradient centrifugation with LSM1077 to get mononuclear cells suspensions and remove dead cells.

Isolation of human thymic epithelial cells

Thymus was cutted in pieces of $3mm^2$ and washed 4 times in RPMI 1640 medium (Invitrogen, Carlsbad, CA, USA). Thymus pieces were digested in medium A (RPMI 1640, collagenase 0.12% (from *Clostridium histoliticum,* Sigma-Aldrich), DNAse I 0.1% (Sigma-Aldrich)) for 15 minutes in a warm bath at 37°C. The supernatant was stored at 4°C and the pieces of thymuses were once again incubated with medium A. This step is renewed 2 times. The 3 supernatants were pooled in the same tube and centrifugated at 1500rpm for 5 minutes. The pellet was resuspended and incubated, with magnetic stirring, in medium B (RPMI 1640, collagenase 0.12% (from *Clostridium histoliticum*), dispase 1.2mg/ml (StemCell Technologies, Grenoble, France), DNAse I 0.1%) for 30 minutes in a warm bath at 37° and then centrifugated at 1500rpm for 5 minutes. The pellet was resuspended with MACS buffer (0.5% BSA, EDTA 2mmol/L pH8, PBS pH7.2), incubated for 10 minutes at 4°C and filtered through 70µm filters. The cells were then sorted to eliminate $CD45^+$ cells (Miltenyi Biotec, Bergisch Gladbach, Germany). The magnetic separation from autoMACS separator (Miltenyi biotec) was used.

Immunofluorescence analysis of thymus sections

Sections of thymuses (6µm) were cut from frozen samples, air dried and fixed in acetone. Then before each step, slides were washed 3 times using PBS (137mM NaCl, 2.7mM KCl, 10 mM Na_2HPO_4, 2mM KH_2PO_4), unless otherwise specified by protocol. After rehydratation in PBS, endogenous peroxidases were quenched with 0.5% H_2O_2 in PBS for 20 minutes. Endogenous biotins were blocked using Endogenous Biotin-Blocking Kit (Molecular Probes, Eugene, OR, USA) following the manufacturer's protocol. Sections were blocked, using Cyanine *3* tyramide signal amplification (TSA) kit (PerkinElmer, Woodbridge, ON, Canada), and labeled with biotin antihuman CD19 antibody (clone HIB19) from BD Biosciences (San

Jose, CA, USA) or biotin antihuman IgM antibody (clone TIBI 82) from Sera-lab (West Sussex, United Kingdom) following the manufacturer protocol. Nuclei were stained with DAPI (4,6 diamidino-2-phenylindole) (Sigma-Aldrich, St Louis, MO, USA). Thymus sections were incubated with 4% paraformaldehyde in PBS for 30 minutes. Coverslips were mounted in DAKO (Sigma-Aldrich) and sealed with nail polish. Images were acquired using a spinning disk confocal microscope (Zeiss® Axio Observer Z1 Yokogawa spinning disk system, objective: Zeiss® Plan-Apochromat 20X/0.8). No bleed-through was detected between channels. Images were stitched to get an overview of the whole tissue and were analyzed using National Institutes of Health Image J software.[E15] In thymic sections, cortico-medullary borders were distinguished by the cellular density visualized by DAPI staining.

Immunofluorescence-AIRE expression

Mononuclear thymic cells suspensions were collected in PBS, after a density gradient centrifugation with LSM1077 to remove dead cells. Unfixed cells (3.10^5) were allowed to adhere for 45 minutes at 37°C in multiwell culture slides (BD Falcon) coated with poly-L-lysine (Sigma-Aldrich). Then before each step, slides were washed 3 times using PBS-1% BSA (Sigma-Aldrich), unless otherwise specified by protocol. The cells were blocked with PBS-1% BSA for 30 minutes at +4°C. Except for wells containing TECs, the cells were labeled with biotin anti-human CD19 antibody (clone HIB19) from BD Biosciences or biotin anti-human IgM antibody (clone TIBI 82) from Sera-lab in BSA-1% BSA for 45 minutes at room temperature followed by an incubation with streptavidine AlexaFluor 647 (Thermo Fisher Scientific, Illkirch, France) in PBS-1% BSA for 30 minutes at +4°C. Cells were then fixed with 2% paraformaldehyde in PBS for 30 minutes and permeabilized with 0.05%Triton X-100 (GE Healthcare Life Sciences) in PBS-1% BSA for 30 minutes. Samples were incubated with anti-AIRE antibody (clone D-17, SantaCruz, Santa Cruz, CA, USA) or goat

IgG (polyclonal, SouthernBiotech AL, USA), as isotype control, in PBS-1%BSA-0.05%Triton-X at 4°C overnight. After 3 washes with PBS-1% BSA-0.05% Triton-X-100, cells were incubated with AlexaFluor 488 donkey anti-goat IgG (polyclonal, Thermo Fisher Scientific) in PBS-1% BSA- 0.05%Triton-X for 1 hour at room temperature. Nuclei were then stained with DAPI (Sigma-Aldrich). Coverslips were mounted in DAKO (Sigma-Aldrich) and sealed with nail polish. Images were acquired using either a spinning disk confocal microscope (Zeiss® Axio Observer Z1 Yokogawa spinning disk system, objective: Zeiss® Plan-Apochromat 20X/0.8 and Plan-Apochromat 100X/1.4) or a laser scanning microscope (Zeiss® Axio Observer Z1, LSM 780 confocal head objective: Zeiss® Plan-Apochromat 63X/1.4). No bleed-through was detected between channels. Images were stitched to get an overview and were analyzed using National Institutes of Health Image J software.[E15]

Flow Cytometry

Cell viability was assessed by incubation of cells with Fixable Viability Dye eFluor® 780 (eBioscience, San Diego, CA, USA) following the manufacturer's protocol. BM and thymic cells' were washed twice in PBE (PBS, 0.5% Bovine Serum Albumine, 2mM EDTA) and resuspended in PBE. Classical surface staining was performed in the dark for 15 minutes at 4°C. Intracellular staining was performed, for Ki67 staining, using Foxp3/Transcription Factor Fixation/Permeabilization Concentrate and Diluent Kit (eBioscience) following the manufacturer's protocol. For PB, BM and thymic B cells of the same individual (P1), the staining was performed using OptiLyse C Lysis Solution (Beckman Coulter, Fullerton, CA, USA) according to manufacturer protocol. The cells were washed twice in PBE buffer and analyzed on a Gallios flow cytometer (Beckman Coulter). Living cells were identified by forward scatter and side scatter gating. Isotypic controls were performed. Data analysis was performed using Kaluza software (Beckman Coulter) with "logicle" compensation.[E16]

For the analysis of protein expression, level the geometric mean fluorescence intensity (MFI) was used. And considering the low numbers of B cells in the thymus, we roughly separated immature and mature B cells on the basis of their CD10 expression.

A comprehensive list of antibodies used for this experiment includes: CD19 APC-AlexaFluor®700 (clone J3-119) was purchased from Beckman Coulter, Ki67 FITC (clone B56), CD3 PC-Cy7 or APC (clone UCHT1), CD5 FITC (clone UCHT2), CD10 PerCP-Cy5.5 (clone HI10a), CD24 FITC or PE (clone ML5), CD27 PE or APC (clone M-T271), CD34 PC7 (clone 581), CD38 PE-CF594 or PC-Cy7 (clone HIT2), CD40 FITC (clone 5C3), CD86 FITC (clone 2331 (FUN-1)), CD138 AlexaFluor®647 (clone MI15), HLA DR/DQ/DP FITC (clone Tu39), IgD PerCP-Cy5.5 (clone IA6-2), IgD FITC (clone IA6-2), IgM FITC (G20-127) and IgM PE-CF594 (G20-127) were purchased from BD Biosciences, CD5-APC-AlexaFluor®750 (clone BL1a) was purchased from Beckman Coulter, IgG PE-Vio770 (clone IS11-3B2.2.3), IgA PerCP-Vio700 (clone IS11-8E10) and IgE PE (clone MB10-5C4) were purchased from Miltenyi Biotec.

Classification of TRAs

As previously described, a protein coding gene was defined as coding for a TRA if its mRNA expression was above 5 times the median (the median expression over all-tissues) in less than 5 tissues.[E17] Each of the following group was considered as a single tissue: (i) all nervous central tissues, (ii) colon and small intestine, and (iii) all testis tissues. Fetal tissues were excluded from the analysis. In addition, a gene was excluded from the TRAs list, if its expression was above 5 times the median in the B cell lineage ($CD19^+$ B cells or B lymphoblast). TRAs identification was performed using the Human U133A/GNF1H Gene Atlas public database[E18] at www.biogps.org.[E19,E20]

According to the list of genes which are induced/repressed in murine B cells, published by Yamano et al.,[E21] the following human genes were selected as AIRE-related genes for quantitative real-time RT-PCR analysis: *SCEL*, *GRIK2*, *LAMP3* and *CDH17* for AIRE-induced genes, and *KLRB1* for AIRE-repressed genes.

Quantitative real-time RT-PCR analysis

$CD3^+CD19^-$ and $CD3^-CD19^+CD27^-IgM^+$ populations were sorted (FACSAria II, BD Biosciences) from thymic mononuclear cells suspensions, of infants undergoing corrective heart surgery, and $CD3^-CD19^+CD27^-IgM^+$ were also sorted from PBMC of healthy donors. Cell viability was assessed with DAPI (Sigma-Aldrich). Purity was controlled after sort (see Fig E4 in this article's Online Repository at www.jacionline.org). RNA was isolated using RNeasy Mini kit (Qiagen, Valencia, CA, USA) following the manufacturer's protocol, including a DNase digest. Reverse transcription was done using High Capacity cDNA Reverse transcription Kit (Applied Biosystems, Foster City, CA) following the manufacturer's protocol, and was performed on a T100™ Thermal cycler (BioRad, Hercules, CA, USA). Preamplification of 10ng of cDNA was performed, with TaqMan® PreAmp Master Mix Kit (Applied Biosystems) on a T100™ Thermal cycler (Biorad). Quantitative real-time PCR reactions were performed on a StepOnePlus realtime thermal cycler (Applied Biosystems) using the TaqMan® Gene Expression Master Mix (Applied Biosystems) following the manufacturer's protocol. Assays were plated in triplicate. Thermal cycling conditions were set at 2 minutes at 50°C and 10 minutes at 95°C, then 40 cycles at 95°C for 15 seconds and 60°C for 1 minute. Relative expression levels were calculated with the comparative Ct method using the mean of the Ct between *GAPDH* and *C1orf43* for normalization.[E22] $CD3^+$ thymic cells or $CD19^+CD27^-IgM^+$ from PBMC were used as calibrator samples. The following list of TaqMan® probes (Applied Biosystems) was used:

GAPDH (Hs02758991_g1), C1orf43 (Hs00367486_m1), *AIRE* (Hs00230829_m1), *KLRB1* (Hs00174469_m1), *CDH17* (Hs00900408_m1), *GRIK2* (Hs00222637_m1), *LAMP3* (Hs00180880_m1), *SCEL* (Hs01557103_m1), *BECN1* (Hs00186838_m1), *ATG5* (Hs00355492_m1).

Whole transcriptome sequencing (RNA-seq)

$CD3^-CD19^+CD27^-IgM^+$ populations were sorted (FACSAria II, BD Biosciences) from thymic mononuclear cells suspensions of infants undergoing corrective heart surgery (n=4), and from PBMC of healthy donors (n=4). Cell viability was assessed with DAPI (Sigma-Aldrich). Purity was controlled after sort (see Fig E4 in this article's Online Repository at www.jacionline.org). RNA was isolated using RNeasy Mini kit (Qiagen) following the manufacturer's protocol, including a DNase digest. Sample quality was assessed using Agilent 2100 bioanalyzer (Agilent Technologies, Palo Alto, CA). Transcriptome libraries preparation and sequencing were performed in the sequencing facility of the IGBMC (Strasbourg, France) using Illumina sequencing platform (Illumina, San Diego, CA). Image analysis and base calling were performed using RTA 2.7.3 and bcl2fastq 2.17.1.14. Reads were mapped onto the hg38 assembly of the human genome using Tophat v2.0.14[E23] and the bowtie v2.1.0 aligner. Gene expression was quantified using HTSeq v0.6.1[E24] and gene annotations from Ensembl release 83. Read counts were normalized across libraries with the method proposed by Anders and Huber.[E25] Comparison between thymic B cells and peripheral B cells gene expression was performed using the method proposed by Love et al.[E26] implemented in the DESeq2 Bioconductor library (v1.6.3). Adjustment for multiple testing was performed with the Benjamini and Hochberg method.[E27] In human thymic B cells 912 genes were induced (168 were TRAs) and 364 genes were repressed (48 were TRAs).

Read normalized and divided by gene length in kb >50; fold-change >4; p-value adjusted for multiple testing <0.05.

Statistical analysis

Statistical comparison between groups was carried out using nonparametric two-tailed Mann-Whitney test. A p-value less than 0.05 was considered as significant. All data were presented as mean ± standard error of the mean (SEM). Tests were applied using Prism 5.0 (GraphPad Software Inc. San Diego, CA).

ACCEPTED MANUSCRIPT

REFERENCES

E1. Real A, Gilbert N, Hauser B, Kennedy N, Shand A, Gillett H, et al. Characterisation of Osteoprotegerin Autoantibodies in Coeliac Disease. Calcif Tissue Int 2015;97:125–33.

E2. Riches PL, McRorie E, Fraser WD, Determann C, van't Hof R, Ralston SH. Osteoporosis associated with neutralizing autoantibodies against osteoprotegerin. N Engl J Med 2009;361:1459–65.

E3. Mappouras DG, Philippou G, Haralambous S, Tzartos SJ, Balafas A, Souvatzoglou A, et al. Antibodies to acetylcholinesterase cross-reacting with thyroglobulin in myasthenia gravis and Graves's disease. Clin Exp Immunol 1995;100:336–43.

E4. Tang J, Yuan J, Hao H. Anti-acetylcholinesterase antibody in myasthenic syndrome. Chin Med J (Engl) 1997;110:698–700.

E5. Phillips TM, Manz HJ, Smith FA, Jaffe HA, Cohan SL. The detection of anti-cholinesterase antibodies in myasthenia gravis. Ann N Y Acad Sci 1981;377:360–71.

E6. Provenzano C, Marino M, Scuderi F, Evoli A, Bartoccioni E. Anti-acetylcholinesterase antibodies associate with ocular myasthenia gravis. J Neuroimmunol 2010;218:102–6.

E7. Marinkovich MP, Taylor TB, Keene DR, Burgeson RE, Zone JJ. LAD-1, the linear IgA bullous dermatosis autoantigen, is a novel 120-kDa anchoring filament protein synthesized by epidermal cells. J Invest Dermatol 1996;106:734–8.

E8. Smith CJA, Bensing S, Burns C, Robinson PJ, Kasperlik-Zaluska AA, Scott RJ, et al. Identification of TPIT and other novel autoantigens in lymphocytic hypophysitis; immunoscreening of a pituitary cDNA library and development of immunoprecipitation assays. Eur J Endocrinol 2012;166:391–8.

E9. Tan FK, Arnett FC, Antohi S, Saito S, Mirarchi A, Spiera H, et al. Autoantibodies to the extracellular matrix microfibrillar protein, fibrillin-1, in patients with scleroderma and other connective tissue diseases. J Immunol Baltim Md 1950 1999;163:1066–72.

E10. Arnett FC, Tan FK, Uziel Y, Laxer RM, Krafchik BR, Antohi S, et al. Autoantibodies to the extracellular matrix microfibrillar protein, fibrillin 1, in patients with localized scleroderma. Arthritis Rheum 1999;42:2656–9.

E11. Pietropaolo M, Castaño L, Babu S, Buelow R, Kuo YL, Martin S, et al. Islet cell autoantigen 69 kD (ICA69). Molecular cloning and characterization of a novel diabetes-associated autoantigen. J Clin Invest 1993;92:359–71.

E12. Gordon T, Grove B, Loftus JC, O'Toole T, McMillan R, Lindstrom J, et al. Molecular cloning and preliminary characterization of a novel cytoplasmic antigen recognized by myasthenia gravis sera. J Clin Invest 1992;90:992–9.

E13. Sasaki H, Kunimatsu M, Fujii Y, Yamakawa Y, Fukai I, Kiriyama M, et al. Autoantibody to gravin is expressed more strongly in younger and nonthymomatous patients with myasthenia gravis. Surg Today 2001;31:1036–7.

E14. Zingaretti C, Arigò M, Cardaci A, Moro M, Crosti M, Sinisi A, et al. Identification of new autoantigens by protein array indicates a role for IL4 neutralization in autoimmune hepatitis. Mol Cell Proteomics MCP 2012;11:1885–97.

E15. Schneider CA, Rasband WS, Eliceiri KW. NIH Image to ImageJ: 25 years of image analysis. Nat Methods 2012;9:671–5.

E16. Tung JW, Heydari K, Tirouvanziam R, Sahaf B, Parks DR, Herzenberg LA, et al. Modern flow cytometry: a practical approach. Clin Lab Med 2007;27:453–468, v.

E17. Pinto S, Michel C, Schmidt-Glenewinkel H, Harder N, Rohr K, Wild S, et al. Overlapping gene coexpression patterns in human medullary thymic epithelial cells generate self-antigen diversity. Proc Natl Acad Sci U S A 2013;110:E3497-3505.

E18. Su AI, Wiltshire T, Batalov S, Lapp H, Ching KA, Block D, et al. A gene atlas of the mouse and human protein-encoding transcriptomes. Proc Natl Acad Sci U S A 2004;101:6062–7.

E19. Wu C, Orozco C, Boyer J, Leglise M, Goodale J, Batalov S, et al. BioGPS: an extensible and customizable portal for querying and organizing gene annotation resources. Genome Biol 2009;10:R130.

E20. Wu C, MacLeod I, Su AI. BioGPS and MyGene.info: organizing online, gene-centric information. Nucleic Acids Res 2013;41:D561–5.

E21. Yamano T, Nedjic J, Hinterberger M, Steinert M, Koser S, Pinto S, et al. Thymic B Cells Are Licensed to Present Self Antigens for Central T Cell Tolerance Induction. Immunity 2015;42:1048–61.

E22. Eisenberg E, Levanon EY. Human housekeeping genes, revisited. Trends Genet 2013;29:569–74.

E23. Kim D, Pertea G, Trapnell C, Pimentel H, Kelley R, Salzberg SL. TopHat2: accurate alignment of transcriptomes in the presence of insertions, deletions and gene fusions. Genome Biol 2013;14:R36.

E24. Anders S, Pyl PT, Huber W. HTSeq--a Python framework to work with high-throughput sequencing data. Bioinforma Oxf Engl 2015;31:166–9.

E25. Anders S, Huber W. Differential expression analysis for sequence count data. Genome Biol 2010;11:1–12.

E26. Love MI, Huber W, Anders S. Moderated estimation of fold change and dispersion for RNA-seq data with DESeq2. Genome Biol 2014;15:550.

E27. Benjamini Y, Hochberg Y. Controlling the False Discovery Rate: A Practical and Powerful Approach to Multiple Testing. J R Stat Soc Ser B Methodol 1995;57:289–300.

FIG E1. A, Flow cytometry analysis, in the lymphoid gate, of thymic (n = 5) and BM (n = 3) $CD19^+$ B cells **B,** Flow cytometry analysis of the different B cells subsets (indicated as a percentage of total $CD19^+$ cells) in thymus ($n \geq 4$) compared to BM (n = 3). Antibodies mentioned on the axes are applied to the population defined on the top of each plot.

FIG E2. B cells ontogeny and markers used for B cell subsets gating strategy.

FIG E3. A, Flow cytometry analysis of $CD19^+$ B cells in thymus, BM and PB of P1. **B** and **C,** Frequency of immature B cells (Fig E3, B) and mature B cells (Fig E3, C) in P1. **D** and **E,** The panels represent respectively B cells MFI of CD86 (Fig E3, D) and CD5 (Fig E3, E) in PB *(red)*, BM *(blue)* and thymus *(black)* for P1.

FIG E4. A, B, C Representative immunostaining of AIRE protein (A, B; *green*) compared to isotype control (C) in TECs. **D, E, F,** Representative immunostaining of AIRE protein (D, E; *green*) compared to isotype control (F) in IgM^+ (*red*) thymic B cells.

FIG E5. Gating strategy and purity of sorted samples. Values are shown as *mean* ± SEM [*minimum and maximum values]* of the percentages of total viable sorted cells in the gates. **A,** Thymuses (n = 5). **B,** PBMC samples (n = 4). **A, B,** Antibodies mentioned on the axes are applied to the population defined on the top of each plot.

ACCEPTED MANUSCRIPT

TABLE E2. List of TRAs expressed in thymic B cells compared to peripheral B cells.

Gene symbol	Gene name	Fold change	Adjusted p-value
NPTX1	neuronal pentraxin I	202.07	1.27E-74
DUSP4	dual specificity phosphatase 4	181.53	1.89E-67
UBE2QL1	ubiquitin-conjugating enzyme E2Q family-like 1	123.92	8.16E-35
TNFRSF11B*[E1,2]	tumor necrosis factor receptor superfamily, member 11b (Aliases OPG; Osteoprotegerin)	94.80	1.19E-84
IGSF3	immunoglobulin superfamily, member 3	92.19	1.36E-29
SYNDIG1	synapse differentiation inducing 1	91.32	5.48E-19
KCNMA1	potassium channel, calcium activated large conductance subfamily M alpha, member 1	89.42	2.68E-52
TFPI2	tissue factor pathway inhibitor 2	88.05	3.81E-20
TNFAIP6	tumor necrosis factor, alpha-induced protein 6	82.93	7.59E-15
KCNK12	potassium channel, two pore domain subfamily K, member 12	80.36	2.98E-131
WNT5B	wingless-type MMTV integration site family, member 5B	72.09	2.48E-34
ACHE*[E3–6]	acetylcholinesterase (Yt blood group)	69.23	2.82E-36
EGR2	early growth response 2	55.72	6.00E-114
GFPT2	glutamine-fructose-6-phosphate transaminase 2	49.48	1.09E-14
CXCL13	chemokine (C-X-C motif) ligand 13	49.33	1.57E-13
GABRA5	gamma-aminobutyric acid (GABA) A receptor, alpha 5	47.82	7.57E-16
NR4A3	nuclear receptor subfamily 4, group A, member 3	43.38	3.38E-38
RAMP1	receptor (G protein-coupled) activity modifying protein 1	41.44	9.93E-10
RGS16	regulator of G-protein signaling 16	41.37	4.51E-64
GADD45G	growth arrest and DNA-damage-inducible, gamma	39.82	9.23E-19
LAD1*[E7]	ladinin 1	39.33	7.92E-12
LHX2	LIM homeobox 2	38.80	1.65E-35
MYO7A	myosin VIIA	37.03	2.87E-15
HR	hair growth associated	34.18	1.40E-09
GATA3	GATA binding protein 3	31.83	6.44E-29
ANLN	anillin actin binding protein	31.18	1.59E-08
ATXN1	ataxin 1	30.76	1.04E-47
RGS13	regulator of G-protein signaling 13	30.48	2.78E-16
RBMS3	RNA binding motif, single stranded interacting protein 3	29.81	4.10E-28
THY1	Thy-1 cell surface antigen	28.94	3.27E-12
SMAD7	SMAD family member 7	27.28	1.69E-74
PCDHGC3	protocadherin gamma subfamily C, 3	22.86	5.24E-45
TULP2	tubby like protein 2	21.17	3.40E-26
ALPL	alkaline phosphatase, liver/bone/kidney	20.89	3.55E-28

ACCEPTED MANUSCRIPT

CDHR1	cadherin-related family member 1	20.71	1.20E-21
OCA2	oculocutaneous albinism II	20.42	7.53E-07
BCAR3	breast cancer anti-estrogen resistance 3	19.93	9.25E-87
BIK	BCL2-interacting killer (apoptosis-inducing)	19.39	4.46E-10
DBNDD2	dysbindin (dystrobrevin binding protein 1) domain containing 2	18.91	2.50E-29
VDR	vitamin D (1,25- dihydroxyvitamin D3) receptor	18.68	2.87E-25
MUC12	mucin 12, cell surface associated	18.00	2.91E-10
PTMS	parathymosin	17.50	5.45E-14
MERTK	MER proto-oncogene, tyrosine kinase	16.29	3.57E-12
ETV5	ets variant 5	15.90	3.97E-20
SCG2*[E8]	secretogranin II	15.07	7.38E-07
LAMP3	lysosomal-associated membrane protein 3	14.17	2.56E-17
WLS	wntless Wnt ligand secretion mediator	13.81	3.43E-06
BCAS1	breast carcinoma amplified sequence 1	13.77	1.71E-25
HBEGF	heparin-binding EGF-like growth factor	13.72	1.08E-13
KLF10	Kruppel-like factor 10	13.52	4.46E-53
VEGFA	vascular endothelial growth factor A	13.10	2.93E-07
BHLHE40	basic helix-loop-helix family, member e40	12.76	5.82E-26
IL6	interleukin 6	12.70	2.93E-27
NINJ1	ninjurin 1	12.68	2.05E-20
ZBED2	zinc finger, BED-type containing 2	12.41	2.20E-16
H1F0	H1 histone family, member 0	12.33	1.81E-11
LRRC32	leucine rich repeat containing 32	12.30	6.94E-12
TNFRSF21	tumor necrosis factor receptor superfamily, member 21	12.07	3.68E-24
SIRPA	signal-regulatory protein alpha	11.83	1.41E-17
SPRY2	sprouty RTK signaling antagonist 2	11.30	7.51E-17
SCAMP5	secretory carrier membrane protein 5	11.27	6.88E-08
PLAU	plasminogen activator, urokinase	11.13	5.45E-09
RRAD	Ras-related associated with diabetes	10.52	7.78E-09
GRAMD1B	GRAM domain containing 1B	10.42	3.57E-11
SLC2A3	solute carrier family 2 (facilitated glucose transporter), member 3	10.22	8.67E-55
MBOAT2	membrane bound O-acyltransferase domain containing 2	10.10	6.92E-28
CETP	cholesteryl ester transfer protein, plasma	9.99	1.98E-12
DHRS9	dehydrogenase/reductase (SDR family) member 9	9.93	7.19E-21
FBN1*[E9,10]	fibrillin 1	9.56	1.10E-19
HACD1	3-hydroxyacyl-CoA dehydratase 1	9.21	2.17E-08
PTPRM	protein tyrosine phosphatase, receptor type, M	8.78	1.86E-07
TP53I3	tumor protein p53 inducible protein 3	8.62	4.83E-49
ARHGEF40	Rho guanine nucleotide exchange factor (GEF) 40	8.41	9.60E-12
LDLRAD4	low density lipoprotein receptor class A domain containing 4	8.30	9.87E-48
HMOX1	heme oxygenase 1	8.22	3.07E-22
MARC2	mitochondrial amidoxime reducing component 2	8.14	4.44E-17
NGFRAP1	nerve growth factor receptor (TNFRSF16) associated protein 1	8.13	1.18E-05

KLK1	kallikrein 1	7.79	1.59E-15
DFNB31	deafness, autosomal recessive 31	7.78	4.56E-33
MFSD2A	major facilitator superfamily domain containing 2A	7.72	2.20E-21
QPCT	glutaminyl-peptide cyclotransferase	7.52	8.13E-10
NMRK2	nicotinamide riboside kinase 2	7.52	8.93E-03
HSPA6	heat shock 70kDa protein 6 (HSP70B')	7.50	1.99E-03
ADAM12	ADAM metallopeptidase domain 12	7.47	1.03E-16
GPR137B	G protein-coupled receptor 137B	7.45	3.16E-35
SYT11	synaptotagmin XI	7.18	1.31E-15
CYBRD1	cytochrome b reductase 1	7.14	1.13E-10
MLF1	myeloid leukemia factor 1	7.07	9.02E-04
TPM2	tropomyosin 2 (beta)	7.03	5.02E-19
GDPD5	glycerophosphodiester phosphodiesterase domain containing 5	7.02	5.31E-12
PLAUR	plasminogen activator, urokinase receptor	6.95	1.41E-04
PLSCR1	phospholipid scramblase 1	6.94	5.12E-24
GPER1	G protein-coupled estrogen receptor 1	6.93	2.49E-13
GCAT	glycine C-acetyltransferase	6.89	1.01E-09
EGR3	early growth response 3	6.86	2.35E-15
GTSF1L	gametocyte specific factor 1-like	6.75	1.86E-12
SYNGR3	synaptogyrin 3	6.66	1.01E-25
B3GALNT1	beta-1,3-N-acetylgalactosaminyltransferase 1 (globoside blood group)	6.63	3.54E-11
ADAMDEC1	ADAM-like, decysin 1	6.52	1.72E-08
AGAP9	ArfGAP with GTPase domain, ankyrin repeat and PH domain 9	6.51	3.13E-12
SEPT5	septin 5	6.50	1.92E-05
ANG	angiogenin, ribonuclease, RNase A family, 5	6.34	4.19E-04
RRAGD	Ras-related GTP binding D	6.22	5.42E-06
JAG2	jagged 2	6.21	3.71E-06
ATF5	activating transcription factor 5	6.06	3.47E-23
CDH17	cadherin 17, LI cadherin (liver-intestine)	6.00	1.27E-5
PSRC1	proline/serine-rich coiled-coil 1	5.97	1.84E-02
ATRNL1	attractin-like 1	5.90	3.08E-06
TIAM1	T-cell lymphoma invasion and metastasis 1	5.88	2.01E-08
C3orf14	chromosome 3 open reading frame 14	5.86	3.25E-07
MYADM	myeloid-associated differentiation marker	5.86	8.25E-15
SEMA4C	sema domain, immunoglobulin domain (Ig), transmembrane domain (TM) and short cytoplasmic domain, (semaphorin) 4C	5.85	2.30E-12
ACOT7	acyl-CoA thioesterase 7	5.73	1.33E-12
ICA1*[E11]	islet cell autoantigen 1, 69kDa	5.72	3.30E-10
SSTR2	somatostatin receptor 2	5.64	1.19E-11
PSD3	pleckstrin and Sec7 domain containing 3	5.59	5.32E-22
SLC35D2	solute carrier family 35 (UDP-GlcNAc/UDP-glucose transporter), member D2	5.55	5.05E-24
C1orf216	chromosome 1 open reading frame 216	5.50	4.62E-21
ZMIZ1	zinc finger, MIZ-type containing 1	5.49	9.73E-54
PER1	period circadian clock 1	5.43	2.24E-10

LRP8	low density lipoprotein receptor-related protein 8, apolipoprotein e receptor	5.41	6.15E-15
FOLR2	folate receptor 2 (fetal)	5.38	9.01E-08
TIE1	tyrosine kinase with immunoglobulin-like and EGF-like domains 1	5.35	5.38E-07
WDR62	WD repeat domain 62	5.33	2.73E-09
SMIM24	small integral membrane protein 24	5.29	2.67E-05
ROR1	receptor tyrosine kinase-like orphan receptor 1	5.11	1.08E-20
INPP1	inositol polyphosphate-1-phosphatase	5.06	3.31E-18
GBP2	guanylate binding protein 2, interferon-inducible	5.03	9.60E-26
HLX	H2.0-like homeobox	4.99	1.35E-16
CYB5R2	cytochrome b5 reductase 2	4.93	4.08E-09
TMEM132A	transmembrane protein 132A	4.92	1.79E-21
LPIN1	lipin 1	4.80	1.00E-27
CSRNP1	cysteine-serine-rich nuclear protein 1	4.75	4.98E-24
PLXNB1	plexin B1	4.74	5.54E-05
BAMBI	BMP and activin membrane-bound inhibitor	4.74	3.73E-08
MS4A4A	membrane-spanning 4-domains, subfamily A, member 4A	4.72	2.31E-04
MMP14	matrix metallopeptidase 14 (membrane-inserted)	4.69	6.63E-04
ANK2	ankyrin 2, neuronal	4.62	7.80E-04
HERC5	HECT and RLD domain containing E3 ubiquitin protein ligase 5	4.59	2.30E-27
RTN2	reticulon 2	4.59	6.66E-05
CYP2J2	cytochrome P450, family 2, subfamily J, polypeptide 2	4.59	2.71E-09
EPS8L1	EPS8-like 1	4.57	6.50E-04
SCN1B	sodium channel, voltage gated, type I beta subunit	4.53	6.70E-06
ZYX	zyxin	4.53	1.03E-24
TUBA1C	tubulin, alpha 1c	4.52	1.14E-06
SPHK1	sphingosine kinase 1	4.49	4.47E-05
STIL	SCL/TAL1 interrupting locus	4.46	3.05E-03
TLN2	talin 2	4.43	5.89E-05
CIT	citron rho-interacting serine/threonine kinase	4.41	5.57E-03
AKAP12* [E12,E13]	A kinase (PRKA) anchor protein 12	4.40	7.01E-08
NAB2	NGFI-A binding protein 2 (EGR1 binding protein 2)	4.38	5.71E-10
PDE9A	phosphodiesterase 9A	4.36	6.26E-07
NET1	neuroepithelial cell transforming 1	4.32	2.17E-14
CISH	cytokine inducible SH2-containing protein	4.28	4.96E-11
ABCG1	ATP-binding cassette, sub-family G (WHITE), member 1	4.27	2.57E-30
NLRP2	NLR family, pyrin domain containing 2	4.26	8.94E-08
PAK6	p21 protein (Cdc42/Rac)-activated kinase 6	4.24	4.01E-06
IZUMO4	IZUMO family member 4	4.22	6.26E-15
CALHM2	calcium homeostasis modulator 2	4.20	4.17E-10
ZDHHC11	zinc finger, DHHC-type containing 11	4.20	2.63E-03
LRRC36	leucine rich repeat containing 36	4.20	1.15E-16
MS4A14	membrane-spanning 4-domains, subfamily A, member 14	4.20	3.88E-13

ACCEPTED MANUSCRIPT

ACCEPTED MANUSCRIPT

FAM101B	family with sequence similarity 101, member B	4.16	4.65E-06
ESR1	estrogen receptor 1	4.16	7.03E-08
METRNL*[E14]	meteorin, glial cell differentiation regulator-like	4.13	1.92E-08
KLF4	Kruppel-like factor 4 (gut)	4.10	2.91E-02
SH2D2A	SH2 domain containing 2A	4.09	1.79E-04
PTP4A3	protein tyrosine phosphatase type IVA, member 3	4.03	6.07E-10

* proteins described as potential autoantigens associated to human autoimmune diseases

[Ex] see Online Repository for supplemental references

ACCEPTED MANUSCRIPT